

## BRAIN TUMOR DETECTION USING SELECTIVE SEARCH AND PULSE-COUPLED NEURAL NETWORK FEATURE EXTRACTION

Brad NIEPCERON, Filippo GRASSIA

*Université de Picardie Jules Verne*

*Laboratoire des Technologies Innovantes (LTI, EA 3899)*

*Avenue des Facultés, Le Bailly*

*Amiens, France*

*e-mail: brad.niepce@gmail.com, filippo.grassia@u-picardie.fr*

Ahmed NAIT SIDI MOH

*Jean Monnet University Saint Etienne*

*LASPI Laboratory – IUT of Roanne*

*Campus Pierre Mendès France*

*20 Av. de Paris, 42300 Roanne Cedex, France*

*e-mail: ahmed.nait@univ-st-etienne.fr*

**Abstract.** The identification of tumorous tissues in the brain based on Magnetic Resonance Images (MRI) analysis is a challenging and time consuming task that highly depends on radiologists expertise. As prompt diagnosis of tumors can often be inherent to the patient’s survival, it is however crucial to decrease the amount of time spent on the manual analysis of MRI while increasing the accuracy of the detection process. To tackle these issues, many research works have already investigated efficient computer vision systems. They offer new opportunities to assist health care providers in the establishment of fast and more accurate tumor detection, classification and segmentation. However, often based on deep learning methods, the development and tuning of these solutions remains time and energy consuming while inducing a lack of explainability in the decision making system. In this study, we respond to these issues by solving a brain tumor detection task using the Selective Search (SS) algorithm coupled with a simplified Pulse-Coupled Neural Network (PCNN) for visual feature extraction and detection validation. The per-

formed experiments showed promising results in terms of computational cost and detection accuracy. This leads to the development of a light-weight brain tumor detection system.

**Keywords:** Biomedical imaging, brain tumor detection, pulse-coupled neural network, selective search, differential evolution

## 1 INTRODUCTION

In recent years, an urgency to assist health-care providers with modern analysis tools appeared with the increasing amount of recorded cases of cancer worldwide and the particular high mortality induced by brain tumors [1]. As the analysis of brain images is a tedious, time consuming and costly process [2], the need for automatic computer-aided diagnosis systems is growing. The diagnosis task performed by radiologist being prone to misinterpretation and up to a 5 % day-by-day error rate [3, 4], assisting their decision making could allow to make early tumor detection more accurate, anticipate a potential therapy and decrease the costs of cancer care. The advances in computer vision and the growth of open-source medical data has brought a major breakthrough in the development of such system based on medical image analysis. Deep learning is one of the most preeminent domain contributing to these advances. It takes the form of Artificial Neural Networks (ANNs) modeling to solve medical vision tasks such as disease detection, unhealthy tissues classification or MRI segmentation. Although, these deep learning based methods seem to be remarkably accurate when solving vision tasks, their development, optimization and generalization still appear to be tedious. Moreover, they bring a few limits that do not make them realistically viable in the medical field.

Firstly, with a dependence to powerful hardware or costly cloud infrastructures [5], they bring along a cost efficiency problem that prevents their deployment in domain with limited resources. As hospitals and clinics always aim to reduce their costs, seeking to incorporate these expensive solutions to their image analysis environment could be very difficult. Secondly, training ANNs for computer vision often requires a need for large datasets [6], which can be hard to find in the medical field because of ethics and privacy protecting patients data. As most of the state-of-the-art medical image analysis methods are supervised, these datasets also need to be labelled, which complicates even more their collection. Finally, deep learning methods face a lack of explainability [7] reflected by the black box property of ANNs that prevent their deployment in domains where the outcomes of a decision making system have to be fully understood. Hence, a replacement or modification of deep learning based methods have to be considered to develop accessible yet powerful computer-aided diagnosis systems meeting the requirements exposed by healthcare providers.

In an attempt to address some of the aforementioned problems, several methods emerged to step towards more viable medical image analysis solutions. Spike based systems for computer vision nowadays appear as good competitors to replace ANNs as they rely on biological models that tackle the lack of explainability and cost efficiency of deep learning methods. Bio-plausible neural networks such as Convolutional Spiking Neural Networks (CSNN) [8] or PCNN [9] are thus being investigated as alternatives to ANNs and the number of studies aiming to use them to build recognition systems is quickly growing. For image processing, the PCNN has been widely studied. Contrary to any other artificial or spiking neural network, it is non-trainable and its synaptic weights remain constant. This behaviour allows such network to output quickly and deal with different tasks without having to modify its structure completely. Studies on its applicability to segmentation and detection tasks were successfully investigated [10, 11]. Mostly developed to perform grayscale image segmentation, some modified PCNN models appeared to increase the range of its applicability and decrease its computational cost. From feature extraction [12] to image fusion [13] the use of such network in the development of fast medical image processing systems is yet to be investigated. Taking advantage of their computational speed, PCNN models can be coupled with Machine Learning classifiers or region-based segmentation methods to create accurate and scalable tumor detection systems. The simple structure of PCNN models also encourages the implementation of medical image analysis processes on cost efficient embedded systems. Our work thus provides an implementation of such system.

In this paper, we first propose an introduction to a PCNN based image processing scheme for MRI sequence fusion and visual features extraction. Then we discuss the development of a brain tumor detection process by coupling the Selective Search (SS) algorithm, the PCNN feature extraction and a distance based validation. Finally, we discuss the optimization of our proposed method with the use of an evolutionary algorithm by tuning the PCNN parameters to fit an objective criteria.

## 2 THE PCNN MODEL

A recent interest for Spiking Neural Networks (SNN) applied to computer vision motivated the investigation of PCNN for medical image processing. By making spatially connected neurons fire together to group pixels with similar intensities, these networks can be particularly efficient for segmentation or clustering tasks. The standard PCNN model is a network of laterally connected neurons, all linked to image pixels. The network is divided into three parts, namely the feeding receptive field, the linking modulation and the pulse generator, as shown in Figure 1. The receptive field part is responsible for the input reception and divides it into a feeding channel  $F_{ij}$  that takes an external and local stimulus and a linking channel  $L_{ij}$  that takes a local stimulus. The input takes the form of a grayscale image  $S_{ij}$  in which each pixel at position  $(i, j)$  is represented by one neuron in the network. The pulsing

process of the PCNN being iterative, the feeding and linking channels dynamics are described by the following equations at the  $n^{th}$  iteration:

$$F_{ij}[n] = \exp^{-\alpha_f} F_{ij}[n - 1] + V_F \sum_{k,l} M_{ij,k,l} Y_{ij}[n - 1] + S_{ij}, \quad (1)$$

$$L_{ij}[n] = \exp^{-\alpha_L} L_{ij}[n - 1] + V_L \sum_{k,l} W_{ij,k,l} Y_{ij}[n - 1] \quad (2)$$

where  $Y_{ij}[n]$  is the output pulse of a neuron,  $M$  and  $W$  are constant synaptic weight matrices and  $(k, l)$  refers to neighboring neurons.  $V_F$  and  $V_L$  are the voltage potential of the channels and  $\alpha_F$ ,  $\alpha_L$  are their attenuation time constants.

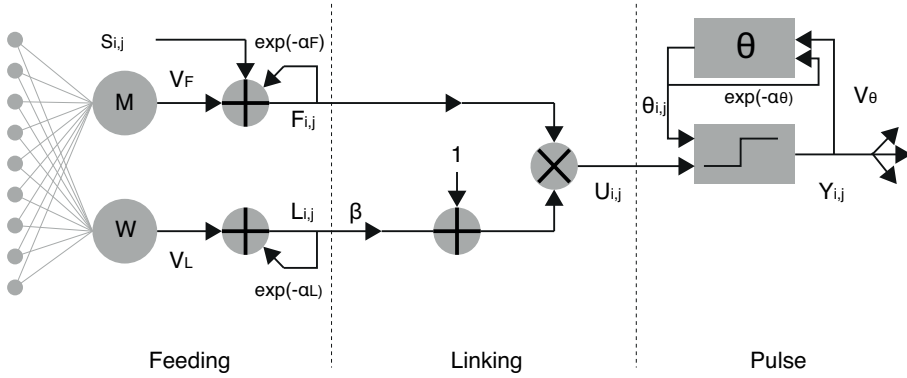


Figure 1. The standard pulse-coupled neural network

In the linking modulation part, both feeding and linking signals are grouped and sent to the internal activity  $U_{ij}$  of the neuron, which is described as:

$$U_{ij}[n] = F_{ij}[n](1 + \beta L_{ij}[n]) \quad (3)$$

where  $\beta$  is the positive linking parameter. Finally, in the pulse generator,  $U_{ij}$  is compared to a dynamic threshold  $\theta_{ij}$  to make the neuron fire by setting  $Y_{ij}$  to 1 if  $U_{ij} > \theta_{ij}$  as:

$$Y_{ij}[n] = \begin{cases} 1, & U_{ij}[n] > \theta_{ij}[n], \\ 0, & \text{otherwise,} \end{cases} \quad (4)$$

$$\theta_{ij}[n] = \exp^{-\alpha_\theta} \theta_{ij}[n - 1] + V_\theta Y_{ij}[n] \quad (5)$$

where  $V_\theta$  and  $\alpha_\theta$  are the voltage potential and the time attenuation constant of the dynamic threshold. This standard form of the PCNN was proven to be efficient for image processing [14] but setting its parameters remains a tedious task to automate.

Some modified versions of it aimed to reduce its amount of parameters to make it suitable for other type of computer vision tasks like classification or image fusion.

### 3 PROPOSED METHOD

If it mostly proved its efficiency towards solving simple binary and multi-channel segmentation tasks, some modification in a PCNN's structure can let it be used to perform different tasks such as image fusion or feature extraction. In this study, we also prove that these models can be coupled with region proposal algorithms to solve tumor detection problems.

#### 3.1 Multi-Channel PCNN Based Medical Image Fusion

Scanning the human body in search of a tumor or any unhealthy group of cells often requires the acquisition of a set of images with different appearances. These sets, also called sequences, are obtained using different radiofrequency pulses and gradients and allow an in-depth analysis of the body part being scanned. The most common types of acquisitions found in open-source brain MRI datasets include the T2-weighted (T2), the T2 Fluid Attenuated Inversion Recovery (FLAIR), T1-weighted (T1) and post-contrast T1-weighted (T1c) sequences. Clinical experts can take advantage of this amount of data by studying each image individually. However, building a computer-aided analysis system taking multiple sequences at the same time can lead to heavy computational workloads. In this work, the BraTS 2020 dataset [15] was used as it comprises all four mentioned sequences along with a ground truth segmentation map for each brain scan. This dataset is composed of pre-operative MRI scans of glioma cases manually segmented by 3 to 4 raters. As it was originally designed as a support to build fully automatic high-grade and low-grade glioma segmentation systems, we extended the dataset by creating ground truth bounding boxes for each MRI slices using the segmentation map provided. These bounding boxes were only set to catch the whole tumor structure as our work did not aim to detect tumor sub-regions.

In computer vision, fusion techniques are used to fasten data processing and analysis, aiming to create one single image out of multiple ones by keeping the amount of information underlying each of them. Some recent works using image fusion in the medical field relied on the use of discrete wavelet transform (DWT) [16, 17]. When using this method, a template sequence first has to be used for reference to match the histograms of the other sequences to it. Then, the sequences are fused by pair and the resulting fused images are fused again until obtaining one single image containing information from all of the latters. This process illustrated in Figure 2 can be time-consuming and does not allow the processing of a large amount of data when facing the availability of limited resources. To replace or improve this method, the m-PCNN [18, 19] was proposed to fusion MRI and Computerized Tomography (CT) scans.

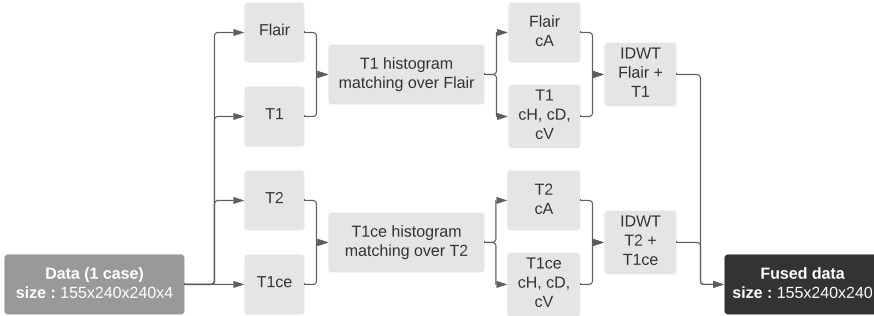


Figure 2. Fusion process of a 4-sequence MRI scan from the BraTS dataset by the discrete wavelet transform

In the m-PCNN the linking modulation is replaced by an information fusion layer that receives multiple inputs and merged them into the internal state of the neuron. This new part is the key behind m-PCNN performances for image fusion as it allows the network to receive multiple input at the same time in the feeding receptive field. While the dynamics of the threshold and the pulse generator are the same as in the standard PCNN model presented above, for a fusion of  $k = 4$  MRI sequences, m-PCNN defines the neuron internal activity  $U_{ij}$  and the fusion channel  $H_{ij}^k$  as:

$$U_{ij}[n] = M^k(Y[n - 1]) + S_{ij}^k, \tag{6}$$

$$H_{ij}[n] = \prod_{k=4}^K (1 + \beta^k H_{ij}^k[n]) + \sigma \tag{7}$$

where  $M^k$  is a weight matrix,  $\beta^k$  is a weighting factor to increase or decrease the importance of one particular sequence during the fusion process.  $\sigma$  is the level factor that controls the average level of the internal activity. Without a linking channel, the m-PCNN is easier to tune than the standard model as it reduces the amount of parameters. In the case of the fusion of our 4 sequences taken from the BraTS dataset, we apply the same parameters as in [19] except for each  $\beta^k$ . Indeed, in order to help the detection process, we first tuned these parameters to let the FLAIR and T2 sequences be more important during the fusion process because they provide higher intensities to voxels representing unhealthy tissues. Note that each scan in the dataset has been registered. Without registration this fusion process would imply the presence of visual anomalies caused by a wrong layering of the images. Figure 3 shows one MRI slice taken from the dataset with all 4 sequences along with the fused image obtained by m-PCNN with  $\{\beta^1, \beta^2, \beta^3, \beta^4\} = \{0.8, 0.3, 0.3, 0.8\}$ , where 1, 2, 3 and 4 corresponds to the FLAIR, T1, T1c and T2 sequences respectively.

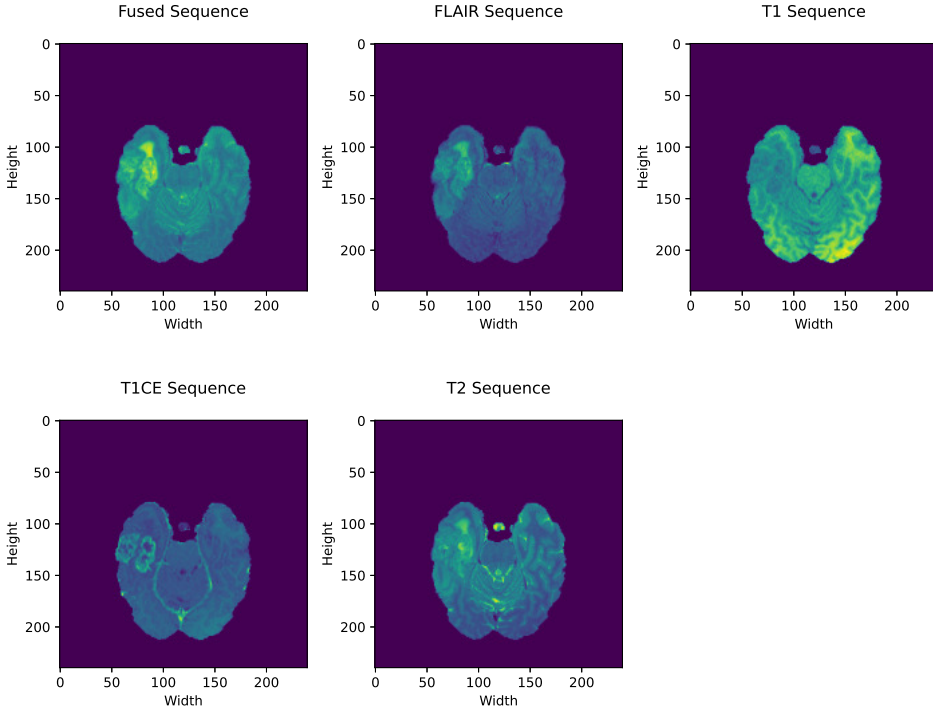


Figure 3. 4 sequences of a random MRI slice taken from the BraTS 2020 dataset and the fused sequence obtain by m-PCNN

### 3.2 Fast-Linking Spiking Cortical Model for Feature Extraction

By keeping track of its pulsing activity, a PCNN model can be used as an efficient feature extraction model [20]. This idea was first introduced by McClurkin et al. [21] in a work where they studied a macaque's neural response to colour and pattern stimuli individually. They discovered the creation of pattern in the subject's brain that were correlated to precise input stimuli. The response to a combination of patterns and colours stimuli was shown to be the multiplication of both individual stimulus. These findings led Johnson [22] to investigate the use of PCNNs to encode images into univariate time series called Image Signatures (IS) composed of the sum of all spikes at each  $n$  iteration. These signatures are specific to shapes that can be found in the image.

This feature extraction method has the advantage of being fast and to provide smaller representation of the original data which can be crucial in environment with limited memory. This makes it particularly interesting to build cost-efficient image analysis systems. An important quality of an IS is that it contains sub-signatures of objects held in the image it represents. Generally, the IS of an image displaying

an object is the summation of the background IS with the object IS. Although this induces a sensitivity to complex background, retrieving the sub-signature that defines a particular object can still be done using the entire image signature. Hence, we assume that PCNNs can be used to retrieve meaningful information in MRI slices in order to build a brain tumor detection system. This is illustrated in Figure 4 in which the signature of an MRI slice from the BraTS dataset is compared with the signature of a sub-region extracted using the ground truth map. The figure shows that the signature obtained from the patch is clearly identifiable within the MRI slice IS and thus motivates the use of IS in brain tumor detection systems. This process was firstly successfully used to solve object recognition tasks [23, 24] by computing the Euclidean distance between a global IS representing the entire image containing the object to detect and local IS representing small patches within the image. This method works well for objects with well defined edges and when a high contrast exist between the background and the object to identify. However, without an optimization scheme for the PCNN parameter tuning and the right strategy to find the right patch size this method appears tedious to adapt to the medical field where the object to detect does not stands out of the background or does not have refined edges.

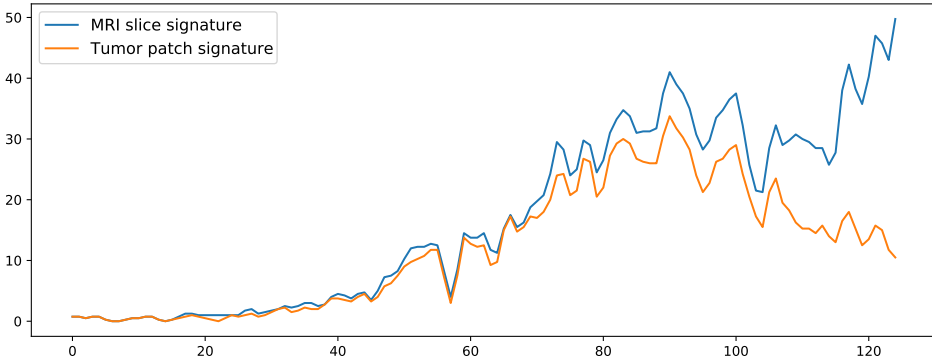


Figure 4. The local image signature of a sub-region containing a tumor compared to the image signature of the MRI slice

To make the parameter initialization easier and build a faster feature extraction model, we proposed the use of a modified version of the standard PCNN called Fast-linking Spiking Cortical Model (FLSCM) [25]. This model is based on the neuronal activity of spiking cortical neurons and combines an external stimulus with a synaptic modulation from neighboring neurons to drive membrane potentials. In this network, the feeding channel and the linking channel are removed and the dynamics of the cortical neuron for IS creation is described as:

$$U_{ij}[n] = \alpha_U U_{ij}[n-1] + S_{ij}(1 + \gamma \sum_{kl} W_{ijkl} Y_{kl}[n-1]), \quad (8)$$

$$\theta_{ij}[n] = \alpha_{\theta}\theta_{ij}[n - 1] + hY_{ij}[n], \tag{9}$$

$$Y_{ij}[n] = \begin{cases} 1, & U_{ij}[n] > \theta_{ij}[n - 1], \\ 0, & \text{otherwise,} \end{cases} \tag{10}$$

$$\theta_{ij}[n] = \theta_{ij}[n - 1] - \delta, \tag{11}$$

$$S[n] = \sum_{ij} Y_{ij}[n] \tag{12}$$

where  $S$  is the obtained image signature.  $\alpha_U$  and  $\alpha_{\theta}$  are the attenuation constants of the membrane potential and the threshold.  $h$  is the refractory period of the neuron and  $\delta$  a decay factor. Here, the linking coefficient  $\gamma$  is defined as a factor of a Laplacian operator. This model allows similar neurons to fire faster and performs better than a standard PCNN. For feature extraction we first implemented this model without a fixed iteration number, instead, the model was ran until every single neuron fired, allowing to represent each pixel intensity group within the obtain signature. By analysing the time series we then set the number of iterations to  $n = 125$  as only after this threshold the neurons associated with low intensities corresponding to healthy tissues were able to fire. A moving average smoothing was also used to remove the noise caused by neurons spiking individually and to enhance the exposition of high intensity pixels. For all the experiments carried in this work, the parameters were set as in [25], creating IS of 258 values before clipping the number of iterations. An example of an IS obtained from an MRI slice using the FLSCM is shown in Figure 5.

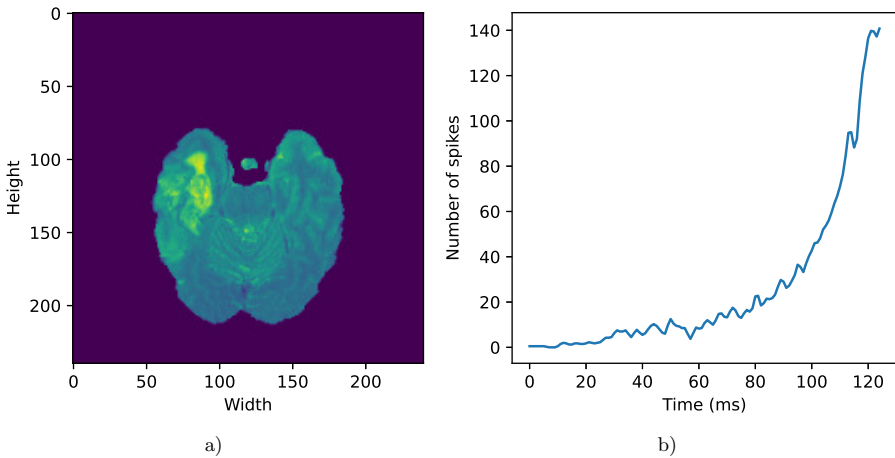


Figure 5. a) An MRI slice and b) its image signature obtained with FLSCM feature extraction

### 3.3 Tumor Detection

A major problem to solve when using PCNN for an object detection task lies in the choice of the right patches to build local signatures. In the work of Gu [23], a sliding window is used to produce the sub-region signatures and find objects contained in the studied images. In this method, the width and height of the window are incremented until a match is found between the local and the global signature. For a tumor detection process, this method appears to be non-viable and counter productive. Indeed, extracting overlapping patches of fixed sizes in each MRI slice would be computationally expensive and would not allow to obtain a pixel perfect detection as the shape of tumors is not necessarily squared. To fit this method to the problem we expose in this work, both width and height of the window should be incremented or decremented at each iteration leading to an even more complex algorithm. Instead, a segmentation based algorithm could be used to extract information out of an MRI slice before computing the detection task.

Region proposal algorithms have gathered attention in deep learning [26] to avoid generating and testing a multitude of sizes for detection bounding boxes. The Selective Search (SS) algorithm [27] is one of them. It relies on a graph-based segmentation method proposed by Felzenszwalb and Huttenlocher [28]. It groups similar parts of the image by using different strategies like colour space and texture analysis. The advantages of the SS for medical image analysis is its computational speed and its ability to create box proposals with different width and height. Using SS for tumor detection allows us to drastically decrease the computational workload of the algorithm and create a faster detection process.

For a complete tumor detection using SS and PCNN feature extraction, the proposed algorithm is thus given as:

**Step 1:** Compute Selective Search on  $M$  to create  $B_{ij}$  bounding boxes.

**Step 2:** Remove boxes with area greater than threshold  $\theta$ .

**Step 3:** Extract image patches  $P_{ij}$  from the boxes.

**Step 4:** Convert each  $P_{ij}$  to signature  $S_{ij}$ .

**Step 5:** Compute the Euclidean distance between each  $S_{ij}$  and the signature  $M_{sign}$  obtained from  $M$ .

**Step 6:** Retain  $B_{min}$  the box that gives the smallest distance  $D_{min}$  as the complete tumor detection box.

Here the threshold  $\theta$  was obtained after experimental observations and by accounting the average volume of a glioma tumor, which is the type of tumor contained in the BraTS dataset. The setting of a threshold allows to eliminate large box candidates and reduce computational cost.

## 4 EXPERIMENTAL STUDY

To evaluate the performances of our proposed detection method, we took a set of MRI cases from the dataset and ran the algorithm on all slices. We ran several experiments to build intuition in the setting of the PCNN parameters during both fusion and feature extraction and analyse their importance during the detection process.

### 4.1 Detection Accuracy and Parameter Tuning

Since our method is not relying on a ground truth to validate the choice of a bounding box, no accuracy evaluation is performed during the detection process. However, in order to prove the efficiency of the model we took advantage of the BraTS dataset and extended it by automatically attaching bounding boxes to each ground truth segmentation map. With this new information, we measured the accuracy of a detection with the Intersection over Union (IoU) metric described as:

$$IoU = \frac{B \cap G}{B \cup G} \quad (13)$$

where B is the predicted bounding box and G the ground truth bounding box. As the detection validation process is mostly based on PCNN models, the importance of parameter tuning was crucial as identifying the tumor's edges is determinant for the right segmented areas to stand out when computing the Felzenszwalb algorithm. Indeed, applying the right over-segmentation can lead to better accuracy as it is often not necessary to create an important amount of segmented areas. Note that further pre-processing operations could be applied to the MRI in order to enhance edge detection and optimize the over-segmentation before the creation of the bounding boxes. An example of correct and false detection using different fusion parameters can be seen in Figure 6. We can see that for a badly fused image, the amount of regions proposed is higher as the fusion process failed to enhance the pixel intensity of the tumorous region. Hence, this bad parameter initialization is also increasing the computational cost of the algorithm as the main IS will have to be compared to every single proposed region.

For this model to aim for better accuracy it is thus crucial to optimize the fusion process. This can be done using an evolutionary algorithm or by simply adding a weight factor to sequences that show high contrasts around the tumor and low ones in any other area of the brain. By setting the parameters manually in some of our experiments we weighted the FLAIR and T2 sequences as explained above, but witnessed that low contrast was the key to creating local IS that will be close enough to global IS to perform an accurate tumor detection. We thus implemented an optimization process based on the Differential Evolution algorithm. It was tested on two different fitness functions, one searching to minimize entropy to induce information gain and an other one to minimize standard deviation (SD) to decrease high contrast present in healthy regions of the brain scan. In our case,

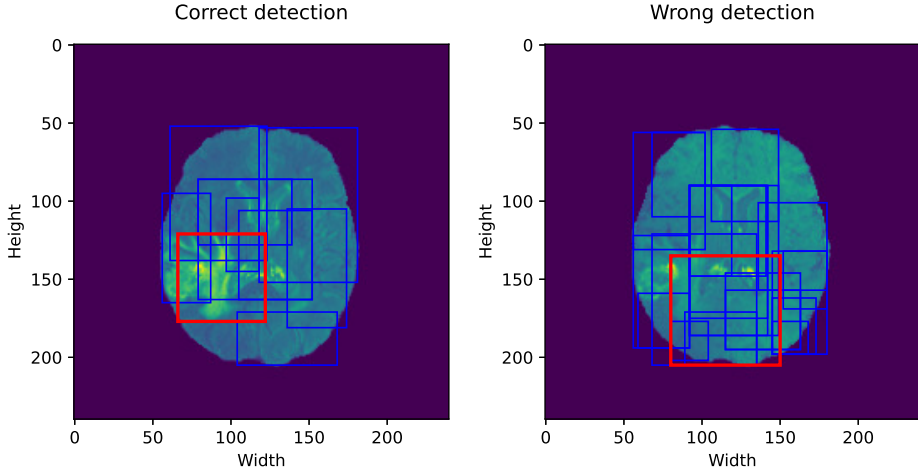


Figure 6. Correct and wrong detection using different fusion parameters. Correct detection parameters:  $\{\alpha_T, v_T, \beta^1, \beta^2, \beta^3, \beta^4, \sigma\} = \{0.015, 20, 0.8, 0.4, 0.4, 0.8, 1.3\}$ . Wrong detection parameters:  $\{\alpha_T, v_T, \beta^1, \beta^2, \beta^3, \beta^4, \sigma\} = \{0.005, 20, 0.3, 0.6, 0.1, 0.8, 1.3\}$ .

minimizing the SD worked better and often induced the  $\beta$  associated with the T1c sequence to be higher than other ones. However, we recorded samples in which a low SD value would not allow the creation of an appropriate IS, in these cases, minimizing the entropy appeared to be a better strategy.

## 4.2 Results and Discussions

Computed on a CPU, the fast bounding boxes proposal provided by Selective Search allowed our algorithm to take 8 seconds on average to perform the detection on each MRI slice when the maximum number of boxes was not set. In other experiments, setting the maximum number of proposals to 10 bounding boxes induced a decrease in the computational time of the algorithm which led to an average of 3 seconds per slice.

This emphasizes the efficiency of our method as it ran relatively fast without the need for GPU power. However, the detection was often not pixel perfect due to the poor amount of pre-processing operations done to the original data. This made the algorithm produce a few inaccurate boxes. Note that we decided not to apply any transformation to each MRI slice to decrease the time needed to perform the entire process. This however proves the performance of PCNN models without alteration on the original data. Figure 7 shows a set of successful detection with their *IoU* score and their ground truth bounding boxes.

Although the methods performed an accurate detection on slices containing medium or large tumor areas, the accuracy when searching for very small tumors in the first and last few slices of each scan appeared to be drastically lower. In

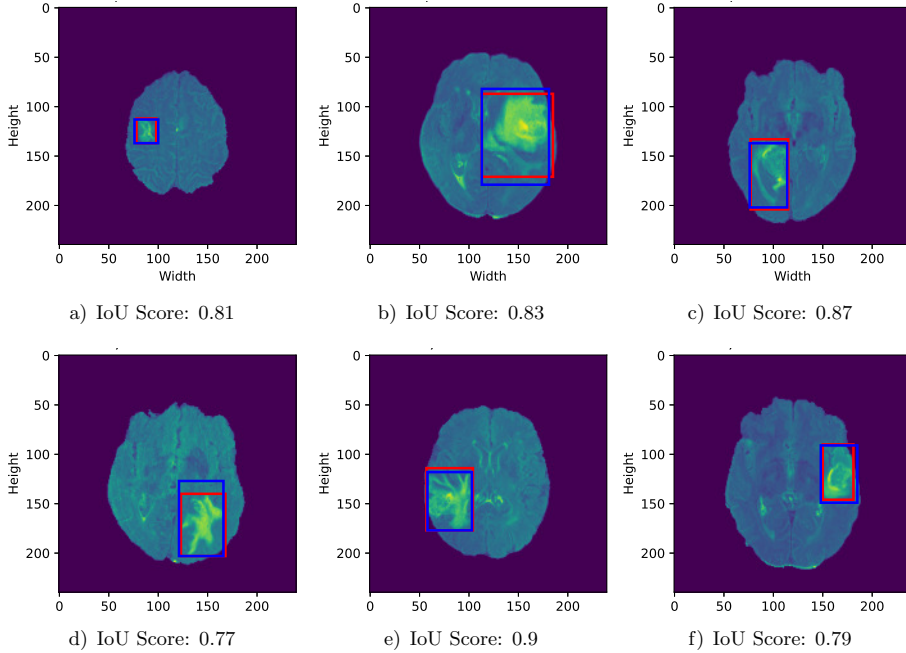


Figure 7. Example of several successful brain tumor detection. The blue box in each image corresponds to the ground truth containing the complete tumor and the red box is the result of our detection method.

fact, these tumorous regions made of only a few voxels can in some cases barely be identified. Since early and late slices are also only made by small spatially independent groups of voxels, comparing the entire image signature to any of these groups would lead to small euclidean distances and thus false the detection process. This also had an effect on the segmentation performed by Selective Search as the variation in all types of similarities computed by the algorithm induced the creation of wrong bounding boxes, this can be seen in Figure 8. Without context around the tumor area the algorithm thus failed to detect it.

For these reasons, the model was evaluated only on slices that provided enough contextual information to distinguish tumorous tissues. Every scan in the BraTS dataset was thus processed by our method and an average *IoU* score of 0.78 was recorded. As the algorithm proposed in our work was kept as simple as possible to obtain low computational workloads we believe some further investigation could come increasing its performances. We first think that some future works could improve the detection score by investigating the use of image pre-processing operations to focus enhancing the contrast between tumorous and healthy tissues in early slices and make the algorithm more sensitive to small clusters of pixels corresponding in the tumor area. A multi-criteria optimization based on a genetic

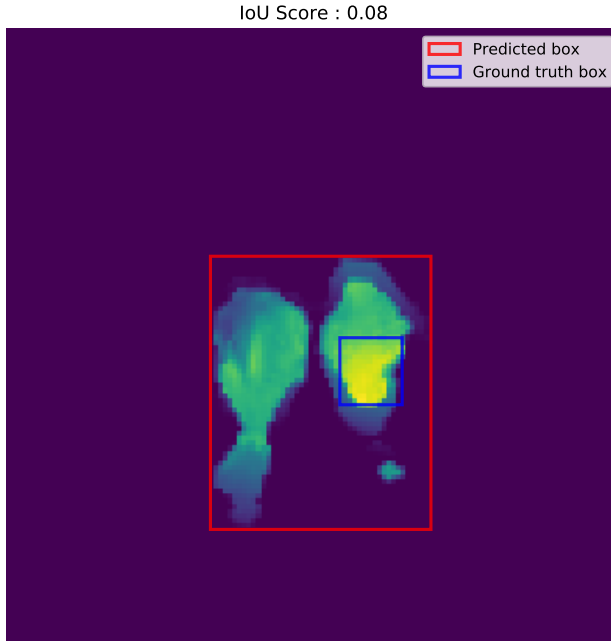


Figure 8. Wrong detection of a tumor in an early slice of a BraTS MRI scan caused by a lack of contextual information

algorithm could also be applied during the fusion process to find a balance between reducing the contrasts by minimizing the SD of the image while minimizing the entropy at the same time or by basing the fitness function on Mutual Information.

Extending this work to a multi-label detection process could also be done by running the algorithm again on the predicted image patches and tuning the fusion process to enhance specific tumorous regions. Our experiments showed that when the fusion process was highly influenced by the T1c sequence, the algorithm was able to detect the boundaries of the core tumor region. In contrast, letting the FLAIR and T2 sequences influence the fusion more than other sequences led to better accuracy in detecting the complete tumor. Note that this approach can only provide meaningful results when the first *IoU* score is highly greater than 0.5. Indeed, a score greater than 0.5 would insure that the majority of the tumor lies within the patch and the algorithm could be used to find inner structures. For that, however, the patch would have to go through the same processing operations as the entire MRI slice before and the PCNN models would have to be retuned. A classifier like the Support Vector Machine could then be used to label each sub-region leading to the creation of a full computer-aided diagnosis system.

## 5 CONCLUSION

In this work, we studied the development of a new method to build a fast and lightweight brain tumor detection system in order to address the limitations brought by most deep learning methods found in the state-of-the-art. Aiming to meet the requirements exposed by healthcare providers in terms of cost efficiency and explainability, we first reviewed the use of the PCNN model for computer vision. We discussed its applicability to image fusion while highlighting the importance of tuning its parameters to increase the performance of the visual task to perform. A modified version of this model was also investigated to produce a feature extraction method and obtain a new representation of an open-source brain image dataset. By coupling this model with the Selective Search algorithm, a region proposal algorithm, we were able to prove the effectiveness and efficiency of our method in performing a complete tumor detection system and gave intuition to enhance the solution by repeating the process to predicted patches for multi-label brain tumor detection and by tuning the fusion process.

We proposed the use of the differential evolution algorithm as a mean to optimize the medical image fusion in order to increase detection accuracy. Although our method exposes some bases to build tumor detection system with PCNN and is perfectible, our results showed that the detection of complete tumors can be done without training a deep neural network and by tuning a simple spike-based model, encouraging the development of fast, light and scalable medical image analysis systems.

## REFERENCES

- [1] SUNG, H.—FERLAY, J.—SIEGEL, R. L.—LAVERSANNE, M.—SOERJOMATARAM, I.—JEMAL, A.—BRAY, F.: Global Cancer Statistics 2020: GLOBOCAN Estimates of Incidence and Mortality Worldwide for 36 Cancers in 185 Countries. *CA: A Cancer Journal for Clinicians*, Vol. 71, 2021, No. 3, pp. 209–249, doi: 10.3322/caac.21660.
- [2] MARIOTTO, A. B.—YABROFF, K. R.—SHAO, Y.—FEUER, E. J.—BROWN, M. L.: Projections of the Cost of Cancer Care in the United States: 2010–2020. *JNCI: Journal of the National Cancer Institute*, Vol. 103, 2011, No. 2, pp. 117–128, doi: 10.1093/jnci/djq495.
- [3] BRUNO, M. A.—WALKER, E. A.—ABUJUDEH, H. H.: Understanding and Confronting Our Mistakes: The Epidemiology of Error in Radiology and Strategies for Error Reduction. *Radiographics*, Vol. 35, 2015, No. 6, pp. 1668–1676, doi: 10.1148/rg.2015150023.
- [4] BERLIN, L.: Radiologic Errors and Malpractice: A Blurry Distinction. *American Journal of Roentgenology*, Vol. 189, 2007, No. 3, pp. 517–522, doi: 10.2214/AJR.07.2209.

- [5] NIEPCERON, B.—NAIT-SIDI-MOH, A.—GRASSIA, F.: Moving Medical Image Analysis to GPU Embedded Systems: Application to Brain Tumor Segmentation. *Applied Artificial Intelligence*, Vol. 34, 2020, No. 12, pp. 866–879, doi: 10.1080/08839514.2020.1787678.
- [6] NAJAFABADI, M. M.—VILLANUSTRE, F.—KHOSHGOFTAAR, T. M.—SELIYA, N.—WALD, R.—MUHAREMAGIC, E. A.: Deep Learning Applications and Challenges in Big Data Analytics. *Journal of Big Data*, Vol. 2, 2015, Art.No. 1, doi: 10.1186/s40537-014-0007-7.
- [7] BIBAL, A.—LOGNOUL, M.—DE STREEL, A.—FRÉNAV, B.: Legal Requirements on Explainability in Machine Learning. *Artificial Intelligence and Law*, Vol. 29, 2021, No. 2, pp. 149–169, doi: 10.1007/s10506-020-09270-4.
- [8] MACHADO, P.—COSMA, G.—MCGINNITY, T. M.: NatCSNN: A Convolutional Spiking Neural Network for Recognition of Objects Extracted from Natural Images. In: Tetko, I., Kůrková, V., Karpov, P., Theis, F. (Eds.): *Artificial Neural Networks and Machine Learning – ICANN 2019: Theoretical Neural Computation*. Springer, Cham, *Lecture Notes in Computer Science*, Vol. 11727, 2019, pp. 351–362, doi: 10.1007/978-3-030-30487-4\_28.
- [9] ECKHORN, R.—REITBOCK, H. J.—ARNDT, M.—DICKE, P.: A Neural Network for Feature Linking via Synchronous Activity: Results from Cat Visual Cortex and from Simulations. In: Cotterill, R. M. J. (Ed.): *Models of Brain Function*. Cambridge University Press, 1989.
- [10] KUNTIMAD, G.—RANGANATH, H. S.: Perfect Image Segmentation Using Pulse Coupled Neural Networks. *IEEE Transactions on Neural Networks*, Vol. 10, 1999, No. 3, pp. 591–598, doi: 10.1109/72.761716.
- [11] YUAN, H.—HOU, G.—LI, Y.: Pulse Coupled Neural Network Algorithm for Object Detection in Infrared Image. *2009 International Symposium on Computer Network and Multimedia Technology*, 2009, pp. 1–4, doi: 10.1109/CNMT.2009.5374517.
- [12] MA, Y.—WANG, Z.—WU, C.: Feature Extraction from Noisy Image Using PCNN. *2006 IEEE International Conference on Information Acquisition*, 2006, pp. 808–813, doi: 10.1109/ICIA.2006.305834.
- [13] QU, X. B.—YAN, J. W.—XIAO, H. Z.—ZHU, Z. Q.: Image Fusion Algorithm Based on Spatial Frequency-Motivated Pulse Coupled Neural Networks in Nonsampled Contourlet Transform Domain. *Acta Automatica Sinica*, Vol. 34, 2009, No. 12, pp. 1508–1514, doi: 10.1016/S1874-1029(08)60174-3.
- [14] CHACON M., M. I.—ZIMMERMAN S., A.—RIVAS P., P.: Image Processing Applications with a PCNN. In: Liu, D., Fei, S., Hou, Z., Zhang, H., Sun, C. (Eds.): *Advances in Neural Networks – ISNN 2007*. Springer, Berlin, Heidelberg, *Lecture Notes in Computer Science*, Vol. 4493, 2007, pp. 884–893, doi: 10.1007/978-3-540-72395-0\_109.
- [15] MENZE, B. H.—JAKAB, A.—BAUER, S.—KALPATHY-CRAMER, J. et al.: The Multimodal Brain Tumor Image Segmentation Benchmark (BRATS). *IEEE Transactions on Medical Imaging*, Vol. 34, 2015, No. 10, pp. 1993–2024, doi: 10.1109/TMI.2014.2377694.
- [16] BHAVANA, V.—KRISHNAPPA, H. K.: Multi-Modality Medical Image Fusion Using

- Discrete Wavelet Transform. *Procedia Computer Science*, Vol. 70, 2015, pp. 625–631, doi: 10.1016/j.procs.2015.10.057.
- [17] SURAJ, A. A.—FRANCIS, M.—KAVYA, T. S.—NIRMAL, T. M.: Discrete Wavelet Transform Based Image Fusion and De-Noising in FPGA. *Journal of Electrical Systems and Information Technology*, Vol. 1, 2014, No. 1, pp. 72–81, doi: 10.1016/j.jesit.2014.03.006.
- [18] WANG, Z.—MA, Y.: Medical Image Fusion Using m-PCNN. *Information Fusion*, Vol. 9, 2008, No. 2, pp. 176–185, doi: 10.1016/j.inffus.2007.04.003.
- [19] ZHAO, Y.—ZHAO, Q.—HAO, A.: Multimodal Medical Image Fusion Using Improved Multi-Channel PCNN. *Bio-Medical Materials and Engineering*, Vol. 24, 2014, No. 1, pp. 221–228, doi: 10.3233/BME-130802.
- [20] LINDBLAD, T.—KINSER, J. M.: *Image Processing Using Pulse-Coupled Neural Networks*. Springer, 1998, doi: 10.1007/978-1-4471-3617-0.
- [21] MCCLURKIN, J. W.—ZARBOCK, J. A.—OPTICAN, L. M.: Temporal Codes for Colors, Patterns, and Memories. In: Peters, A., Rockland, K.S. (Eds.): *Primary Visual Cortex in Primates*. Springer, Boston, MA, Cerebral Cortex, Vol. 10, 1994, pp. 443–467, doi: 10.1007/978-1-4757-9628-5\_11.
- [22] JOHNSON, J. L.: Time Signatures of Images. *Proceedings of 1994 IEEE International Conference on Neural Networks (ICNN '94)*, Vol. 2, 1994, pp. 1279–1284, doi: 10.1109/ICNN.1994.374368.
- [23] GU, X.—WANG, Y.—ZHANG, L.: Object Detection Using Unit-Linking PCNN Image Icons. In: Wang, J., Yi, Z., Zurada, J. M., Lu, B. L., Yin, H. (Eds.): *Advances in Neural Networks – ISNN 2006*. Springer, Berlin, Heidelberg, Lecture Notes in Computer Science, Vol. 3972, 2006, pp. 616–622, doi: 10.1007/11760023\_91.
- [24] GU, X.: Feature Extraction Using Unit-Linking Pulse Coupled Neural Network and Its Applications. *Neural Processing Letters*, Vol. 27, 2008, No. 1, pp. 25–41, doi: 10.1007/s11063-007-9057-6.
- [25] ZHAN, K.—SHI, J.—LI, Q.—TENG, J.—WANG, M.: Image Segmentation Using Fast Linking SCM. *2015 International Joint Conference on Neural Networks (IJCNN)*, IEEE, 2015, pp. 1–8, doi: 10.1109/IJCNN.2015.7280579.
- [26] HE, K.—GKIOXARI, G.—DOLLÁR, P.—GIRSHICK, R. B.: Mask R-CNN. *2017 IEEE International Conference on Computer Vision (ICCV)*, 2017, pp. 2980–2988, doi: 10.1109/ICCV.2017.322.
- [27] UIJLINGS, R. R.—VAN DE SANDE, K. E. A.—GEVERS, T.—SMEULDERS, A. W. M.: Selective Search for Object Recognition. *International Journal of Computer Vision*, Vol. 104, 2013, No. 2, pp. 154–171, doi: 10.1007/s11263-013-0620-5.
- [28] FELZENSZWALB, P. F.—HUTTENLOCHER, D. P.: Efficient Graph-Based Image Segmentation. *International Journal of Computer Vision*, Vol. 59, 2004, No. 2, pp. 167–181, doi: 10.1023/B:VISI.0000022288.19776.77.



**Brad NIEPCERON** received his Ph.D. in computer science from the University of Picardie Jules Verne (UPJV), France. His research interests mainly focus on developing and improving computer vision systems based on deep learning and computational neurosciences to tackle the energy and cost problems of their use in the medical field. He has been involved in several research projects on artificial intelligence (AI) related topics and is self-employed to develop AI-based solutions for medical image analysis and global environmental issues.



**Filippo GRASSIA** received his M.Sc. degree in computer science engineering from Catania University (Italy) in 2006 and his Ph.D. degree in electronic engineering from the Bordeaux University (France) in 2013. From January 2013 to August 2014 he was involved in the European Brain-Bow project as CNRS post-doctoral fellow in the IMS Laboratory, working on experimental and theoretical studies to design neuromorphic chip for brain repair that will reproduce the functional organization of a damaged part of the central nervous system. Since 2014, he is Associate Professor of the University of Picardie Jules Verne,

teaching lessons, from the first year to master courses, of analog and digital electronics, system on chip and signal processing. His research interests are focused on neuromorphic engineering and complex systems principles applied to robotics, stochastic neuronal computations, neuronal noise on hardware, chaos and nonlinear time series analysis, bifurcation analysis, neuron models, parameter estimation, metaheuristic algorithm, and fixed point calculations.



**Ahmed NAIT SIDI MOH** is Full Professor at the Jean Monnet University (UJM), Saint Etienne, France. He received the Ph.D. degree in computer science and automatic control from the University of Technology of Belfort (UTBM), Belfort, France, in 2003. He was Assistant Professor at the UTBM from 2004 to 2011. After, he joined as Associate Professor the University of Picardie Jules Verne (UPJV), Amiens, France, where he obtained his Habilitation à diriger des Recherches (HDR) in computer engineering in 2016. He is the author of several articles published in international journals, conferences, and workshops.

He is involved in several national and international events such as conferences and workshops organization, technical program committee member of many international journals and conferences; participation to national research groups. His research has been supported by many research and development projects including European grants, regional projects, and EU EACEA Erasmus Mundus projects. He is interested in research topics in the field of healthcare and industrial engineering, with problems of modeling, analysis and control, performance evaluation, resources sharing, optimization, scheduling and interoperability for service composition, information and communication technologies.